DMD Fast Forward. Published on March 24, 2006 as doi:10.1124/dmd.105.009035

Comparison of mouse and rat cytochrome P450 mediated metabolism in liver and intestine

Marcella Martignoni[1], Geny Groothuis[2] and Ruben de Kanter[1,b]

Preclinical Development, Nerviano Medical Sciences, Nerviano, Milan, Italy (M.M., R.d.K.);

Groningen University Institute for Drug Exploration (GUIDE), Dept. Pharmacokinetics & Drug Delivery, Groningen, the Netherlands (G.G.)

Running title: CYP in rat and mouse intestine

Corresponding author:

Marcella Martignoni

Preclinical Development

Nerviano Medical Sciences

Viale Pasteur 10,

20014 Nerviano (MI), Italy.

Phone: +39-0331-581228

Fax: +39-0331-581105

E-mail: marcella.martignoni@nervianoms.com

Number of text pages: 32

Number of tables: 4

Number of figures: 3

Number of references: 22

Number of words in

abstract: 245

introduction: 654

discussion: 1486

Abbreviations:

CYP, cytochrome P450; NADPH, β-nicotinamide adenine dinucleotide phosphate reduced form; RT-PCR, real-time quantitative reverse transcription-polymerase chain reaction; MEGX, monoethylglycinexylidide; Nor-verapamil, normethyl-verapamil; DMSO, dimethylsulfoxide; TOH, hydroxytestosterone; dNTP, 2'- deoxynucleoside 5'-triphosphate; dATP, 2'-deoxyadenine 5'-triphosphate; dGTP, 2'-deoxyguanine 5'-triphosphate; dTTP, 2'-deoxythymine 5'-triphosphate; dCTP, 2'-deoxycytosine 5'-triphosphate; BSA, bovine serum albumin; LC-MS/MS, liquid chromatography coupled to tandem mass spectrometry.

ABSTRACT

The liver is considered to be the major site of first-pass metabolism, but also the small intestine is able to contribute significantly. The improvement of existing and the development of new *in vitro* techniques, such as intestinal slices, allow a better understanding of the intestine as a metabolic organ. In this paper, the formation of metabolites of several human CYP3A substrates by liver and intestinal slices from rat and mouse was compared. The results show that liver slices exhibited a higher metabolic rate for the majority of the studied substrates, but some metabolites were produced at a higher rate by intestinal slices, when compared with liver slices. Co-incubation with ketoconazole inhibited the metabolic conversion in intestinal slices almost completely but inhibition was variable in liver slices. In order to better understand the role of CYP3A in mice, we studied the relative mRNA expression of different CYP3A isoforms in intestine and liver from mice because in this species CYP3A expression has not been well described in these organs. It was found that in mice CYP3A13 is more expressed in the intestine, while CYP3A11, CYP3A25 and CYP3A41 are more expressed in the liver, comparable to similar findings in the rat. All together, these data demonstrate that, in addition to liver, the intestine from mouse and rat may have an important role in the process of first-pass metabolism, depending on the substrate. Moreover, we show that intestinal slices are a useful *in vitro* technique to study gut metabolism.

INTRODUCTION

Although it is widely believed that the liver is the major site of first-pass metabolism, recent studies have indicated that the small intestine is able to contribute significantly to the overall first-pass metabolism of many drugs. Apart from the metabolic capacity, there are several other factors that play a role in the contribution of the intestine to the first pass effect of drugs. Firstly, the intestine is exposed to high concentrations of orally administered xenobiotics (Doherty and Charman, 2002). Secondly, anatomically the small intestine has a serial relationship with the liver in the process of absorption being the anterior organ. Thirdly, in addition to drug metabolizing enzymes such as cytochrome P450 (CYP) isoenzymes, also efflux proteins, such as P-glycoprotein and multidrug-resistance associated proteins, present in the apical membrane of the enterocytes, influence the metabolism process by recycling drugs between enterocytes and lumen with the consequent higher drug exposure to intestinal metabolic enzymes (Doherty and Charman, 2002). Thus, the amount of an orally administered drug that reaches the systemic circulation can be reduced by both intestinal and hepatic metabolism. For some substrates, it has even been suggested that the role of intestinal metabolism is quantitatively greater than that of hepatic metabolism in the overall first-pass effect (Wu et al., 1995; Paine et al., 1996). Therefore, the important question is raised which factors determine the role of intestinal metabolism in the first-pass effect.

The contribution of the small intestine to overall drug metabolism is difficult to evaluate clinically because the organs are perfused in series. Therefore, to obtain a better understanding of the role of the intestine, especially in human drug metabolism, an *in vitro* technology is very

much needed. Intestinal microsomes have been used to study intestinal metabolism, but their major drawback is that metabolic activity is at least partly lost during preparation due to the presence of proteases, with the consequent underestimation of the role of the intestine (Emoto et al., 2000a). Other laboratory techniques, available to study first pass-metabolism, include everted sacs, which also loose their tissue integrity as they require, for metabolic activity, artificial NADPH generation system to be present (Emoto et al., 2000b). Further, some (but not all) single drug metabolizing isoenzymes are commercially available but upscaling to the organ activity is not straightforward due to non-physiological co-substrate concentrations, and lack of interaction with other enzymes and of intercellular communication. Therefore, to overcome these problems, we selected intestinal slices as *in vitro* tool, taking advantage of the maintenance of the tissue integrity and the relatively simple and straightforward preparation technique suitable to different species (de Kanter et al., 2005; Martignoni et al., 2004). Rat and mouse were selected because they are extensively used in toxicology and pharmacology studies. In particular, athymic nude mice (nu/nu) were chosen because they are commonly used in tumour growth inhibition research (Kelland, 2004). In human, but also in laboratory animal species, cytochrome P450 3A (CYP3A) appears to be the major drug metabolizing enzyme sub-family in intestine (Emoto et al., 2000a; McKinnon et al., 1995). Therefore a set of human CYP3A substrates was selected and incubated with intestinal and liver slices of rat and mouse and with rat intestinal microsomes in order to compare their metabolic rates between different organs and between different *in vitro* models. Inhibition by ketoconazole, a CYP inhibitor, was included to confirm the role of CYP mediated metabolism. A scaling factor was determined in order to be able to compare the data of microsomes and slices. Slice viability during incubation was assessed by measuring ATP content in both liver and intestinal slices. In addition, we compared the relative mRNA expression levels

of CYP3A11, CYP3A13, CYP3A25 and CYP3A41 in mouse liver and intestine, by using real-time RT-PCR, in order to better understand the role of these organs in CYP3A-mediated metabolism. Knowledge about CYP3A mRNA expression in intestine has been described for the rat (Matsubara et al., 2004), but still is lacking for the mouse.

MATERIALS AND METHODS

Chemicals. The following compounds were obtained from the sources indicated: dimethylsulfoxide (DMSO), D -glucose, gentamicin sulphate, midazolam, ketoconazole, lidocaine, carbamazepine, quinidine, verapamil, 1-OH-triazolam, carbamazepine epoxide, normethyl-verapamil were from Sigma-Aldrich (St. Louis, MO, USA). Testosterone was from Fluka (Buchs, Switzerland). Testosterone metabolites, 3-OH-quinidine, 1-OH and 4-OH-midazolam were from Ultrafine Chemicals (Manchester, UK). MEGX was from Astra (Soderstaije, Sweden). Triazolam was from Pharmacia (Kalamazoo, MI, USA). Williams' Medium E, amphotericin B, 5x first strand buffer, RnaseOUT, Superscript, dATP, dGTP, dCTP, dTTP, random hexamer primers, DTT and BSA were obtained from Gibco (Paisley, Scotland, UK). RNA 6000 Nano Assay was from Agilent Technologies (Palo Alto, CA, USA). RiboGreen™ RNA Quantitation kit was from Molecular Probes (Eugene, OR, USA). Qiagen RNAeasy® mini kit was from Qiagen Ltd (Crawley, UK). RNAlater™ was from Ambion (Austin, TX, USA). TaqMan® Universal PCR Master Mix Reagents, SYBR® Green PCR Master Mix, and TaqMan® probes were obtained from Applied Biosystems (Foster City, CA, USA). The oligonucleotide primers were synthesized by Nerviano Medical Sciences Labs (Nerviano, Milano, Italy). ATPlite kit was from PerkinElmer (Boston, USA). Protein assay kit was from Bio-Rad (München, Germany). Male intestinal rat microsomes were from Xenotech (Lenexa, KS, USA).

Animals. Sprague Dawley male rats and male nude mouse were obtained from Charles River (Como, Italy) and were maintained under a 12-h light/dark cycle, with free access to

drinking water. Nude mice were fed with 4RFN food pellets that are enriched in protein and lipid content and sterilized by γ-irradiation, while rats received standard 4RF21 pellets (Mucedola, Settimo Milanese, MI, Italy). Animals were housed in standard cages with bedding but for nude mice the air supply was filtered using EPA filters to protect the nude mice against infections.

Liver and intestinal slice preparation. After i.p. anaesthesia with sodium thiopental 100 mg/kg (rat) and a cocktail of ketamine (67 mg/kg), xylazine (15 mg/kg) and acepromazine (1 mg/kg) (mouse), the livers and the first 25-30 cm intestine (thus mainly duodenum of the small intestine) were excised and stored in ice-cold Williams' Medium E until use (max. 0.5 h). Liver slices (diameter 8 mm) were prepared in ice-cold Williams' Medium E that was oxygenated with 95% O_2 / 5% CO_2 and supplemented with extra glucose (25 mM), using a Krumdieck tissue slicer as described elsewhere (Martignoni et al., 2004). The slices obtained were subsequently stored in ice-cold Williams' Medium E until use (within 0.5 h after the preparation).

Agarose filled and embedded slices were prepared as described elsewhere (de Kanter et al., 2005). Shortly, the excised 25 cm of the small intestine was first cut in two parts that were subsequently ligated on one side. These parts were then filled with 3% (w/v) low melting agarose solution in 0.9% (w/v) NaCl at 37°C and allowed to gel in ice-cold Williams' Medium E. The agarose-filled intestine was cut in 1 cm parts and these were embedded in the agarose solution at 37°C using the Tissue Embedding Unit from Alabama R&D (Munford, AL, USA) and allowed to gel so that agarose gel cylinders with a diameter of 16 mm were formed. These cylinders were used to prepare precision-cut intestinal slices, with a diameter of 16 mm and a thickness of about 0.25 mm, using a Krumdieck tissue slicer as described above for liver slices. When the slices were transferred to the incubation plates, the agarose surrounding the slices was separated from the slice, so that only the ring of intestinal tissue (diameter about 3-5 mm) was used.

Culture of liver slices. Slices were individually incubated in 6 well culture plates (3.2 ml Williams' Medium E, liver slices) or in 12 well culture plates (1.3 ml Williams' Medium E, intestinal slices) under 95% O_2 / 5% CO_2 at 37°C and supplemented with glucose (25 mM) and gentamicin (50 μg/ml). For intestinal slices, also amphotericin B (2.5 μg/ml) was added. Liver and intestinal slices were incubated in triplicate with 100 μM of the following substrates: testosterone, triazolam, quinidine, lidocaine, carbamazepine, verapamil and midazolam. The compounds were dissolved in DMSO (100 mM) so that the final concentration of organic solvent was 0.1%. Test compounds were also co-incubated in the presence of 10 μM ketoconazole, to further characterize the role of CYP. Incubation period was 3 hours and at different time points (0, 10, 20, 30, 60, 90 and 180 min) a medium aliquot (80 μl) was removed and added to an equal volume of ice-cold acetonitrile. At the end, the slices were disrupted using a MSE Ultrasonic disintegrator (Fisons, Loughborough, UK) to check the amount of metabolites trapped inside the slices. For all the substrates, apart from testosterone, no differences between slice homogenate and slice medium was observed (data not shown).

LC-MS/MS analysis. After centrifugation at 5000 g for 20 min, the samples were analyzed by LC-MS/MS. For testosterone only, 1 ml homogenate was extracted with 6 ml of dichloromethane. After removal of the water phase and protein interphase, the organic solvent was evaporated and testosterone and its metabolites were dissolved in 1 ml organic phase. The supernatants of centrifuged samples were analyzed by LC-MS/MS, using a Turbo Ion Spray source and a Triple Quadrupole API 4000 instrument (Perkin-Elmer, Woodbridge, Canada). A 4.6 (inner diameter) x 12.5 mm C_8 column (Zorbax - Agilent Technologies) was applied. A mobile phase containing 10 mM ammonium formate (pH 4.0) and acetonitrile was used; for all

compounds but testosterone, acetonitrile was increased from 5% to 95% within 0.4 min and then back to 5% in 1.4 min. The flow rate was 1.5 ml/min for the first 0.2 min to equilibrate the column quickly and 0.2 min after injection the flow rate was reduced to 0.6 ml/min. For testosterone, acetonitrile in the eluents was increased from 5% to 50% during the first 6 min using a flow of 0.5 ml/min and then back to 5% in 2 min. After injection of 20 µl of the sample, ion spectra were acquired in positive mode and the quantification was performed by comparing the peak areas with authentic standards of each metabolite. The results are expressed as pmol/min/mg protein using data obtained in the time-span that metabolites formation rates were linear in time (30 min for triazolam, quinidine, lidocaine, carbamazepine, verapamil, 20 min for midazolam in both liver and intestine slices and 20 min and 180 min for testosterone in liver slices and intestine slices, respectively). The protein content was determined for each intestinal slice using the BioRad Protein assay Kit.

Rat intestinal microsomes incubation. Male intestinal rat microsomes (Xenotech, Lenexa, KS, USA) were incubated at a concentration of 0.5 mg protein/ml in 100 mM phosphate buffer at pH 7.4 at 37°C, in the presence of 100 µM of the substrates as described for slices at 37°C. The reactions were started by the addition of the co-factor NADPH (final concentration: 1 mM). At different time points (0, 10, 20, 30 and 45 min) an aliquot (80 µl) was removed and the reaction was terminated by the addition of equal volume of ice-cold acetonitrile. All incubations were performed in duplicate. Analysis was performed using LC-MS/MS, as described above.

Rat intestinal microsomes preparation for the determination of the scaling factor.

Four small samples (~1 g) from rat intestine were weighed and homogenized in a known volume (~ 5 ml) of 100 mM phosphate containing 150 mM KCl and 1 mM EDTA, pH 7.4, using a Potter

homogenizer. An aliquot of the homogenate was used for the determination of the total amount of the protein. Microsomes were prepared from the homogenate by centrifugation (100000 g for 90 min) of the post-mitochondrial supernatant (9000 g for 20 min). The microsomal pellet was resuspended in buffer and centrifuged again at 100000 g for 90 min. Microsomes were resuspended in about 1 ml 100 mM phosphate buffer containing 150 mM KCl, and stored in aliquots of 0.1 ml at -80°C. The protein concentration of the microsomes and of the homogenate was determined using the Bio-Rad Protein assay kit.

ATP content. The ATP content of slices incubated in parallel was determined as described before (de Kanter et al., 2005) using the ATPLite-M kit from Perkin Elmer (Boston, MA, USA) and a TopCount NXT Luminescence Instrument from Perkin Elmer (Boston, MA, USA).

RNA preparation from liver and intestinal samples. Tissue samples (~ 30 mg) of liver, duodenum, ileum and colon were taken from three male nude mice after anaesthesia as described above and stored in RNAlater™ at 4°C. Total RNA was extracted from the tissue using QIAGEN RNeasy® mini kit. The quality of the isolated RNA was assessed using RNA 6000 Nano Assay and the Agilent 2100 bioanalyzer. RNA concentration was determined using a RiboGreen™ RNA Quantitation kit.

Reverse transcription. The mixture was prepared as follows: 1x first strand buffer, 64 units RNAseOUT, 200 units Superscript, 0.6 mM of dNTP (dATP, dGTP, dCTP and dTTP), 0.75 μg random hexamer primers, 10 mM DTT and 16 ng BSA. To this mixture 1 μg of total extract RNA was added. The reverse transcription reaction was performed for 10 min at 25°C, 60 min at 42°C and 30 min at 37°C.

Design of primers and probes. The cDNA sequences of mouse CYP3A11, CYP3A13, CYP3A25, CYP3A41 and β-actin were obtained from GenBank accession numbers: NM 007818.2, NM 007819.1, NM 019792.1, NM 017396.1 and NM 007393. PCR primers and probe sequences were designed using PrimerExpress software (Applied Biosystems) and shown in Table 1. Nucleotide primers and probe sequences were checked against the NCBI BLAST database to ensure specificity for the selected gene.

Real- time quantitative PCR. Real-time quantitative PCR was performed, employing an iCycler iQ™ Real time PCR detector system (Bio-Rad). The PCR reaction was performed in a 96 well plate. The reaction mixture (13.5 μl) was added in each well to give the following concentrations: 1x master mix reagents, 200-900 nM of each primer and 200 nM probe for each cyp mRNA assay. cDNA (1.5 μl) was added to each well and the final volume was 15 μl. The thermal cycle condition was 50°C for 2 min, 95°C for 10 min to activate Amplitaq Gold DNA polymerase, denaturation at 95°C for 15 sec and anneal/extension at 59°C for 1 min (40 cycles). Quantitative PCR for β-actin mRNA was also performed to normalize for RNA loading.

Statistical analysis. All data are given as means ± SEM and are average values from three values per experiment; experiments were repeated either two or three times. Statistical evaluation among groups was carried out using two-tailed Student's *t*-test, and $p < 0.05$ was considered significant.

RESULTS

Viability of slices. To determine the viability of intestinal and liver slices during incubation, ATP levels were assessed directly after preparation of the slices and after incubation with and without ketoconazole. In rat liver slices, ATP was maintained during incubation with a slight increase at 3 hours (Fig. 1A). In rat intestinal slices, ATP levels dropped during the first 30 min of incubation and then remained constant until three hours of incubation (Fig. 1B). No effect of addition of ketoconazole (10 μM) was found on ATP levels in both rat liver and intestinal slices (Fig. 1A and 1B).

Metabolite formation by liver and intestinal slices from rats. Both rat liver and intestinal slices showed extensive metabolism of testosterone towards several metabolites. The metabolite formation expressed per mg of protein per minute by liver slices was respectively 2-fold (androstenedione) 3-fold (6β-TOH) and 6-fold (16α-TOH) higher in comparison to intestinal slices (Fig. 2A). 7α-TOH and 2α+2β-TOH were detected in rat liver slice incubations, but not in intestinal slices. In contrast, 16β-TOH formation appeared to be higher in intestinal slices than in liver slices (7-fold). Also 3-OH-quinidine formation was 3-fold higher in intestinal slices than in liver slices, but the formation of carbamazepine epoxide was higher in liver slices in comparison to intestinal slices (7-fold). The formation of metabolites of lidocaine, verapamil, midazolam and triazolam was not significantly different between slices from liver and intestine when expressed per mg protein (Fig. 2A). The ratio of activity in liver/intestine is given in Table 2.

Incubation of intestinal slices with 10 μM ketoconazole inhibited the formation of the metabolites from all compounds tested for more than 80%, apart from androstenedione formation

that was inhibited for 50%. In liver slices the percentage of inhibition varied from 0% to100 %, depending on the substrate (Fig. 3A).

Determination of a microsomal scaling factor. To be able to compare the rate of metabolism between intestinal microsomes to intestinal slices a microsomal scaling factor was determined. Starting from four small pieces, the protein content of intestinal rat tissue was determined directly after homogenization, and was 47 ± 6.0 mg protein/g intestinal tissue. After intestinal microsomes preparation, the yield of the microsomal protein recovered was determined, which was 2.1 ± 0.2 mg protein/g intestinal tissue. To convert microsomal metabolic rate from activity per mg microsomal protein to activity per mg of intestinal protein, microsomal metabolic rates were multiplied by the scaling factor 2.1/47 = 0.05 in order to compare with intestinal slice metabolism.

Drug metabolism by rat intestinal microsomes. The metabolic activities by intestinal slices and intestinal rat microsomes calculated per mg intestinal protein using the scaling factor of 0.05 are shown in Table 3. The metabolic rates in intestinal slices were significantly higher for all substrates studied (3-29 fold) when compared to the metabolic rates in microsomes.

Metabolite formation by liver and intestinal slices from mice. Also using slices from mouse liver and intestine, testosterone gave rise to the formation of several metabolites such as 6β-TOH, 16α-TOH, 16β-TOH, and androstenedione in both liver and intestine, but in contrast to rat, no 7α-TOH was found. 2α+2β-TOH was found in liver slices, but not in intestine slices. Metabolite formation was respectively 8-fold (androstenedione), 11-fold (16α-TOH) and 5-fold (16β-TOH) higher in liver slices (Fig. 2B). There were no significant differences observed in the metabolite formation of 6β-TOH, 1-OH-triazolam, 3-OH-quinidine, and nor-verapamil

between liver and intestine. Significantly higher was the formation of MEGX (4-fold formation), carbamazepine epoxide (6-fold formation) and 1-OH- and 4-OH-midazolam (2-fold formation for both 1-OH and 4-OH-hydroxylation) in mouse liver slices (Fig. 2B and Table 2).

Like it was shown for rat, incubation of mouse intestinal slices with 10 μM ketoconazole inhibited the formation of the metabolites of all compounds tested more than 80%, apart from androstenedione formation that was inhibited for 50%. In mouse liver slices the percentage of inhibition varied from 0% to 100 %, depending on the substrate (Fig. 3B).

Detection of CYP3A mRNA levels in mouse liver and intestine. In rats, the expression of CYP3A isoforms in liver and intestine has been described (Matsubara et al., 2004), whereas in mice this information is still lacking. Therefore, to be able to better interpret differences in metabolic rates between liver and intestine, we investigated their relative mRNA expression in mouse liver and intestine. Due to the absence of RNA standards in the current study, expression of the investigated isoforms can be compared among tissues (liver versus intestine of the same species), but not between the different isoforms. In both mouse liver and intestine, the major mouse CYP3A isoforms (CYP3A11, CYP3A13, CYP3A25 and CYP3A41) were detected. CYP3A11 (6%), CYP3A25 (10%) and CYP3A41 (5%) were less expressed in duodenum compared to liver (Table 4). CYP3A11 (2%), CYP3A25 (4%) and CYP3A41 (2%), were detected in ileum at lower level than in liver. On the contrary, CYP3A13 was more expressed in the intestine (202% in duodenum and 103% in ileum) than in liver. For each of the CYP3A isoforms the expression in the ileum was 30-50% lower than in duodenum (CYP3A11: 38%, CYP3A13: 51%, CYP3A25: 35% and CYP3A41: 34%). In colon, CYP3A13 was the only

CYP3A isoform detected at appreciable level (46% of liver value), whereas the other isoform were less than 0.1% when compared to liver (Table 4).

DISCUSSION

In this study, the metabolic properties of liver and intestine were compared *in vitro* by using liver and intestinal slices from both rat and mouse. Consistent with the knowledge that CYP3A4 is the main isoform of P450 family in the human intestine (Emoto et al., 2000a) and that CYP3A4 is responsible for the oxidative metabolism of 50% of drugs currently on the market (de Wildt et al., 1999), we selected a set of marker substrates which are known to be metabolized by human CYP3A.

The feasibility of liver and intestinal slices for metabolism studies was shown before (Martignoni et al., 2004; de Kanter et al., 2005; van de Kerkhof et al., 2005). In both liver and intestinal slices, ATP levels were maintained at a satisfactory level during incubation (Fig. 1), although a drop of ATP content was measured after the first 30 min incubation in intestinal slices. We have also observed this phenomenon in earlier studies (de Kanter et al., 2005), where we showed that ATP levels *in vivo* (about 2 nmol ATP/mg protein) and the ATP content in intestinal slices during incubation were comparable. The increase ATP level at time zero is still unexplained but may be ascribed to ATP synthesis at 4°C in the oxygenated media (de Kanter et al., 2005). The superiority of intestinal slices over intestinal microsomes as a model for metabolic studies was demonstrated when the same substrates were incubated with both *in vitro* preparations. The metabolic rate expressed per mg total intestinal protein was significantly higher using slices for all metabolic conversions studied (Table 3). The difference in metabolite rates between slices and microsomes ranged 3-29-fold between substrates. This dissimilarity may be explained assuming the involvement of different isoforms with different stability. Also, the involvement of transporters that may take up or extrude the compounds into and out of the cells at a different

rate may help to explain those differences. We conclude from the higher metabolic capacity that intestinal slices are a more appropriate *in vitro* model to study gut metabolism than intestinal microsomes, although only a proper *in vitro- in vivo* comparison can give a definitive answer on whether the higher metabolic rates as observed with intestinal slices are closer to the *in vivo* situation.

Incubation of liver and intestinal slices with the selected human CYP3A substrates shows that both liver and intestine participate in metabolism of these substrates in both species, although to a different extent, depending on the substrate (Fig. 2A for rat and Fig. 2B for mouse). In general the metabolite formation rate is quite similar for both species. Differences were observed for the formation of androstenedione (~ 5-fold), 6β-TOH (~ 2-fold), 16α-TOH (~ 2-fold) and 2α+2β-TOH (~ 4-fold) being higher in mouse liver than rat liver. In addition, 7α-TOH testosterone was not detected in mouse liver slices.

With respect to the ratio of liver to intestine activities considerable species differences were found: 16β-TOH and 3-OH-quinidine formation rates were significantly higher in intestine slices in comparison to liver slices in rat, but not in mouse. This was due to the lower metabolic activity in rat liver compared to mouse liver. For most of the metabolites the formation rates was higher in liver than in intestine but the ratio liver/intestine varied between the species (Table 2). This indicates that this ratio cannot be simply extrapolated between species.

To confirm the role of CYP in both the intestinal and the hepatic metabolism, slices were incubated with ketoconazole, a broad rat CYP inhibitor (Kobayashi et al., 2003). In the clinic, ketoconazole affects largely the pharmacokinetics of drugs that are primarily metabolized by CYP3A4, resulting in a substantial decrease of first-pass metabolism (Moody et al., 2004). In intestinal slices from both mouse and rat, ketoconazole strongly inhibited the metabolism of all

tested compounds, whereas in liver the inhibitory effect was more variable. This means that *in vivo*, drug-drug interactions such as by ketoconazole may occur both in liver and intestine, which results in higher exposure to the parent compound. In addition, we hypothesize that metabolite formation of the tested substrates in intestinal slices is mainly mediated by CYP1A and CYP3A isoforms in rat because those two isoforms are mostly expressed in rat intestine (Kaminsky and Zhang, 2003) and by CYP3A in mouse, because until now this isoform is the only CYP found to be present in mouse intestine (Emoto et al., 2000a). In liver slices, however, no complete inhibition was reached with ketoconazole, suggesting that metabolism can be attributed not only to CYP1A and CYP3A but also to other CYPs enzymes, which are apparently little expressed in rat and mouse intestine. For example, it is known that CYP2D participates in lidocaine N-deethylation in rats (Wan et al., 1997), but CYP2D is little expressed in rat intestine (Aiba et al., 2003). Also hepatic metabolism of midazolam in mouse, yielding 1-OH and 4-OH metabolites, has, apart from CYP3A, a significant CYP2C component (Perloff et al., 2000) and mouse and rat intestine appear to have very low CYP2C expression (Emoto et al., 2000b; Kaminsky and Zhang, 2003). In rats, apart from CYP3A1, also CYP1A1 and CYP2B1 were detected in enterocytes, while CYP2C11, CYP2A1, CYP2B2, CYP2E1, CYP3A2 and CYP4A1, which are expressed in liver, were not detectable in intestine by using RT-PCR and immunoblot analysis (Kaminsky and Zhang, 2003). On the other hand, it was reported that in rats, CYP2C6, CYP2C11, CYP2B1, CYP2D1 and CYP1A1 are expressed in duodenum, jejunum and ileum at least at the mRNA level (Lindell et al., 2003). In addition, previous studies revealed that rat CYP3A isoforms are expressed differently between liver and intestine and that some CYP3A substrates are metabolized by different isoforms in those two organs (Matsubara et al., 2004 ; Takara et al., 2003). Rat CYP3A1 and CYP3A2 are expressed predominantly in liver and are not, detectable in

the intestinal tract, whereas CYP3A9 and CYP3A18 are detectable in both liver and intestine. Earlier it was found that, in rat, CYP3A9 was 3-fold more expressed in duodenum than in liver and CYP3A18 was 16-fold more expressed in duodenum than in liver (Matsubara et al., 2004). In contrast, CYP3A62 has been reported to be the predominant form in rat intestinal tract, being 9-fold more expressed in duodenum in comparison to liver (Matsubara et al., 2004). This different expression in CYP3A isoforms between liver and intestine in rats may explain the differences in formation rates of CYP3A metabolites between liver and intestine as was found in this study (Fig. 2A). However, if for example the higher expression of CYP3A62 in rat intestine is responsible of the observed higher 3-OH-quinidine and 16β-OHT formation in rat (Fig. 2A) can only be speculated at this moment. Another explanation for this difference is that the biotransformation reactions studied are not mainly catalyzed by CYP3A isoenzymes, as is suggested by different inhibition profile by ketoconazole in liver slice incubations, compared to intestinal slice incubations (Fig. 3A and 3B). Here, we show that similar to rats (Matsubara et al., 2004), mouse CYP3A isoenzymes are expressed differently between liver and intestine. Mouse CYP3A11, CYP3A25 and CYP3A41 are predominantly expressed in the liver, whereas CYP3A13 is more detected in the intestine than in liver (Table 4). In man, CYP3A4/5 is the most expressed CYP isoform in the small intestine (McKinnon et al., 1995), while CYP1A1, CYP2C19 and CYP2D6 are less expressed isoforms (Doherty and Charman, 2002). Together, this indicates that both in human, mouse and rats the intestine, expressing a different CYP profile than liver (including different CYP3A isoforms), may play a unique role in the metabolism of xenobiotics and may contribute to first-pass metabolism to a different extent than the liver. In addition species differences in liver/intestine ratio's of enzyme activities make inter-species extrapolation hazardous.

Another observation was that, in mice, the mRNA expression of CYP isoforms decreased along the mouse intestinal tract, from duodenum to colon, which is in accordance with earlier findings in rat (Matsubara et al., 2004) and man (de Waziers et al., 1990). Also CYP-mediated enzyme activities were recently shown to decrease along the intestinal tract, using rat intestinal slices (van de Kerkhof et al., 2005).

The current study underlines the potential of intestinal slices to study intestine metabolism *in vitro* and, consequently, to predict drug-drug interactions (Kanazu et al., 2005). Because the preparation of slices is basically the same for each species, we expect that slices from other species including human can also be used to predict intestinal metabolism. This *in vitro* model to study (human) gut metabolism is of interest considering that no other relatively simple models that maintain tissue architecture are available. More investigations are needed to further characterize the role of the intestine in first-pass metabolism such as the investigation of a broader range of marker substrates covering different CYP isoenzymes, and the effect of different inhibitors. Besides, a comparison between *in vitro* and *in vivo* data would allow a better estimation and prediction of the role of the intestine.

ACKNOWLEDGEMENTS

The authors are grateful to Grazia Saturno and to Elena Barbaria for the PCR design and to Anna Moscone for the excellent technical support to LC-MS/MS analyses.

REFERENCES

Aiba T, Takehara Y, Okuno M and Hashimoto Y (2003) Poor correlation between intestinal and hepatic metabolic rates of CYP3A4 substrates in rats. *Pharm Res* **20:**745-748.

de Kanter R, Tuin A, van de Kerkhof E, Martignoni M, Draaisma AL, de Jager MH, de Graaf IA, Meijer DK and Groothuis GM (2005) A new technique for preparing precision-cut slices from small intestine and colon for drug biotransformation studies. *J Pharmacol Toxicol Methods* **51:**65-72.

de Waziers I, Cugnenc PH, Yang CS, Leroux JP and Beaune PH (1990) Cytochrome P 450 isoenzymes, epoxide hydrolase and glutathione transferases in rat and human hepatic and extrahepatic tissues. *J Pharmacol Exp Ther* **253:**387-394.

de Wildt SN, Kearns GL, Leeder JS and van den Anker JN (1999) Cytochrome P450 3A: ontogeny and drug disposition. *Clin Pharmacokinet* **37:**485-505.

Doherty MM and Charman WN (2002) The mucosa of the small intestine: how clinically relevant as an organ of drug metabolism? *Clin Pharmacokinet* **41:**235-253.

Emoto C, Yamazaki H, Yamasaki S, Shimada N, Nakajima M and Yokoi T (2000a) Characterization of cytochrome P450 enzymes involved in drug oxidations in mouse intestinal microsomes. *Xenobiotica* **30:**943-953.

Emoto C, Yamazaki H, Yamasaki S, Shimada N, Nakajima M and Yokoi T (2000b) Use of everted sacs of mouse small intestine as enzyme sources for the study of drug oxidation activities in vitro. *Xenobiotica* **30:**971-982.

Kaminsky LS and Zhang QY (2003) The small intestine as a xenobiotic-metabolizing organ. *Drug Metab Dispos* **31:**1520-1525.

Kanazu T, Okamura N, Yamaguchi Y, Baba T and Koike M (2005) Assessment of the hepatic and intestinal first-pass metabolism of midazolam in a CYP3A drug-drug interaction model rats. *Xenobiotica* **35:**305-317.

Kelland LR (2004) Of mice and men: values and liabilities of the athymic nude mouse model in anticancer drug development. *Eur J Cancer* **40:**827-836.

Kobayashi K, Urashima K, Shimada N and Chiba K (2003) Selectivities of human cytochrome P450 inhibitors toward rat P450 isoforms: study with cDNA-expressed systems of the rat. *Drug Metab Dispos* **31:**833-836.

Lindell M, Lang M and Lennernas H (2003) Expression of genes encoding for drug metabolising cytochrome P450 enzymes and P-glycoprotein in the rat small intestine; comparison to the liver. *Eur J Drug Metab Pharmacokinet* **28:**41-48.

Martignoni M, Monshouwer M, de Kanter R, Pezzetta D, Moscone A and Grossi P (2004) Phase I and phase II metabolic activities are retained in liver slices from mouse, rat, dog, monkey and human after cryopreservation. *Toxicol In Vitro* **18:**121-128.

Matsubara T, Kim HJ, Miyata M, Shimada M, Nagata K and Yamazoe Y (2004) Isolation and characterization of a new major intestinal CYP3A form, CYP3A62, in the rat. *J Pharmacol Exp Ther* **309:**1282-1290.

McKinnon RA, Burgess WM, Hall PM, Roberts-Thomson SJ, Gonzalez FJ and McManus ME (1995) Characterisation of CYP3A gene subfamily expression in human gastrointestinal tissues. *Gut* **36:**259-267.

Moody DE, Walsh SL, Rollins DE, Neff JA and Huang W (2004) Ketoconazole, a cytochrome P450 3A4 inhibitor, markedly increases concentrations of levo-acetyl-alpha-methadol in opioid-naive individuals. *Clin Pharmacol Ther* **76:**154-166.

Paine MF, Shen DD, Kunze KL, Perkins JD, Marsh CL, McVicar JP, Barr DM, Gillies BS and Thummel KE (1996) First-pass metabolism of midazolam by the human intestine. *Clin Pharmacol Ther* **60:**14-24.

Perloff MD, von Moltke LL, Court MH, Kotegawa T, Shader RI and Greenblatt DJ (2000) Midazolam and triazolam biotransformation in mouse and human liver microsomes: relative contribution of CYP3A and CYP2C isoforms. *J Pharmacol Exp Ther* **292:**618-628.

Takara K, Ohnishi N, Horibe S and Yokoyama T (2003) Expression profiles of drug-metabolizing enzyme CYP3A and drug efflux transporter multidrug resistance 1 subfamily mRNAS in small intestine. *Drug Metab Dispos* **31:**1235-1239.

van de Kerkhof EG, de Graaf IA, de Jager MH, Meijer DK and Groothuis GM (2005) Characterization of rat small intestinal and colon precision-cut slices as an in vitro system for drug metabolism and induction studies. *Drug Metab Dispos* **33:**1613-1620.

Wan J, Imaoka S, Chow T, Hiroi T, Yabusaki Y and Funae Y (1997) Expression of four rat CYP2D isoforms in Saccharomyces cerevisiae and their catalytic specificity. *Arch Biochem Biophys* **348:**383-390.

Wu CY, Benet LZ, Hebert MF, Gupta SK, Rowland M, Gomez DY and Wacher VJ (1995) Differentiation of absorption and first-pass gut and hepatic metabolism in humans: studies with cyclosporine. *Clin Pharmacol Ther* **58:**492-497.

Footnotes

Corresponding author:

Marcella Martignoni, Preclinical Development, Nerviano Medical Sciences, Viale Pasteur 10, 20014, Nerviano, (Milan), Italy.

Addresses authors:

Marcella Martignoni[1], Geny Groothuis[2] and Ruben de Kanter[1,b]

[1] Preclinical Development, Nerviano Medical Sciences, Viale Pasteur 10, 20014 Nerviano (MI), Italy.

[2] Groningen University Institute for Drug Exploration (GUIDE), Dept. Pharmacokinetics & Drug Delivery, Ant. Deusinglaan 1, 9713 AV Groningen, the Netherlands.

[b] Present address: Solvay Pharmaceuticals, C.J. van Houtenlaan 36, 1381 CP Weesp, the Netherlands.

Figure Legends

Fig. 1. ATP levels in rat liver slices (Fig. 1A) and rat intestinal slices (Fig. 1B) during incubation time with and without 10 μM ketoconazole.

Results are means of individual slices (two separate experiments, n=3 slices each) ± SEM.

Fig. 2. Drug metabolite formation by liver and intestinal rat (Fig. 2A) and mouse (Fig. 2B) slices.

100 μM of substrates (testosterone, triazolam, quinidine, lidocaine, carbamazepine, verapamil and midazolam) were incubated for three hours with liver and intestinal rat slices. Results are means of individual slices (three separate experiments, n=3 slices each) ± SEM. Values significantly different between liver and intestinal slices: $^{*}p < 0.05$.

n.d., not detectable

Fig. 3. Inhibitory effect of ketoconazole in liver and intestinal rat (Fig. 3A) and mouse (Fig. 3B) slices.

100 μM of substrates (testosterone, triazolam, quinidine, lidocaine, carbamazepine, verapamil and midazolam) were co-incubated with and without 10 μM ketoconazole for three hours. Results are means of individual slices (three separate experiments, n=3 slices each) ± SEM.

The bar for 7α-TOH and 2α+2β-TOH was omitted because no formation was detected in intestinal slices.

§ The formation of 16α-TOH and 16β-TOH (in mouse liver slices) and of 2α+2β-TOH (in both mouse and rat liver slices) was not inhibited by ketoconazole.

DMD Fast Forward. Published on March 24, 2006 as DOI: 10.1124/dmd.105.009035
This article has not been copyedited and formatted. The final version may differ from this version.

Table 1

Taqman® primer and probe sequences of mouse cyp mRNA

Gene	Primers/Probes	5' → 3' Sequence	Amplicon Size (bp)
CYP3A11	Forward	TCACACACACAGTTGTAGGGAGAA	64
	Reverse	GTCCATCCCTGCTTGTTTGTC	
	Probe	ACAGAGAAGTAAATTGC	
CYP3A13	Forward	ACCGGCGGCGCTTT	59
	Reverse	ATTCTCAGAGATAGAGATGGCCTTTT	
	Probe	TCCAGTGGGTATTTTG	
CYP3A25	Forward	CTTCACTGTCCAGCCTTGTGAA	61
	Reverse	AATTGGTTCCCTGCTGATCTTC	
	Probe	AGACACAGATCCCCC	
CYP3A41	Forward	GGTTGTACCACGGGATGTAGTTATAA	95
	Reverse	TCTGATGTTCTTAGACACTGCCTTTC	
	Probe	TCAAGGAGTTCTGCTGAGTT	
β-actin	Forward	TTCTTTGCAGCTCCTTCGTT	75
	Reverse	GACCAGCGCAGCGATATC	

Table 2

Ratio's of metabolic activities in liver and intestine slices from rat and mouse.

Metabolites measured	**Activity ratio liver/intestine**	
	rat	**mouse**
androstenedione	1.5	8.3
MEGX	1.7	4.3
6β-TOH	3.4	2.3
16α-TOH	5.5	11
16β-TOH	0.1	4.8
nor-verapamil	0.9	0.8
3-OH-quinidine	0.3	1.1
1-OH-triazolam	1.4	0.8
4-OH-midazolam	2.2	1.8
1-OH-midazolam	0.7	1.7
carbamazepine epoxide	6.6	5.8

100 μM of substrates (testosterone, triazolam, quinidine, lidocaine, carbamazepine, verapamil and midazolam) were incubated for three hours with liver and intestinal slices from rat and mouse. Results are ratio's from means of individual slices (three separate experiments, n=3 slices each).

DMD Fast Forward. Published on March 24, 2006 as DOI: 10.1124/dmd.105.009035
This article has not been copyedited and formatted. The final version may differ from this version.

Table 3

Metabolite formation by rat intestinal slices and rat intestinal microsomes.

Metabolites measured	**microsomes** pmol/min/mg microsomal protein	**microsomes** pmol/min/mg total intestinal protein (after scaling)	**slices** pmol/min/mg total intestinal protein	**ratio** slices / microsomes
androstenedione	425 ± 25	21 ± 1.2	126 ± 25	6.0
MEGX	76 ± 9.6	3.8 ± 0.5	101 ± 14	27
6β-TOH	110 ± 16	5.5 ± 0.8	25 ± 2.0	4.5
16α-TOH	41 ± 6.7	2.0 ± 0.4	7.8 ± 0.81	3.9
16β-TOH	46 ± 8.4	2.3 ± 0.4	10 ± 1.3	4.3
nor-verapamil	171 ± 27	8.5 ± 1.3	53 ± 7.5	6.2
3-OH-quinidine	61 ± 1.0	3.0 ± 0.05	88 ± 7.8	29
1-OH-triazolam	108 ± 3.0	5.4 ± 0.1	17 ± 3.5	3.1
4-OH-midazolam	80 ± 15	4.0 ± 0.8	11 ± 3.0	2.8
1-OH-midazolam	114 ± 17	5.7 ± 0.9	26 ± 6.4	4.6
carbamazepine epoxide	14 ± 3.0	0.7 ± 0.1	5.5 ± 0.98	7.9

100 μM of substrates (testosterone, triazolam, quinidine, lidocaine, carbamazepine, verapamil and midazolam) were incubated with both rat intestinal slices and rat intestinal microsomes. Results are means of individual slices (three separate experiments, n=3 slices each) or individual microsomes incubations (two separate experiments, n=3 incubations each) ± SEM. Results from intestinal microsomes were corrected using the scaling factor between microsomes and slices (see text).

Table 4

Relative amounts (arbitrary units of CYP3A mRNA/μg total RNA) of CYP3A mRNA in liver and intestine of male mouse.

	Cytochrome P450			
	CYP3A11	**CYP3A13**	**CYP3A25**	**CYP3A41**
Liver	5.4 ± 1.07	0.56 ± 0.12	5.28 ± 1.38	11.9 ± 2.9
Duodenum	0.32 ± 0.08 (6%)	1.13 ± 0.33 (202%)	0.55 ± 0.09 (10%)	0.65 ± 0.18 (5%)
Ileum	0.12 ± 0.07 (2%)	0.58 ± 0.29 (103%)	0.19 ± 0.05 (4%)	0.22 ± 0.14 (2%)
Colon	0.001 ± 0.0003 (0.02%)	0.26 ± 0.08 (46%)	0.0068 ± 0.004 (0.12%)	0.004 ± 0.001 (0.03%)

The percentage mRNA of the corresponding CYP isoforms detected in liver is given between brackets. Total RNA (3.5 ng) was loaded for real-time RT-PCR assay and the levels of CYP mRNA were corrected by β-actin mRNA expression to normalize RNA loading. Results are means of three animals ± SEM.

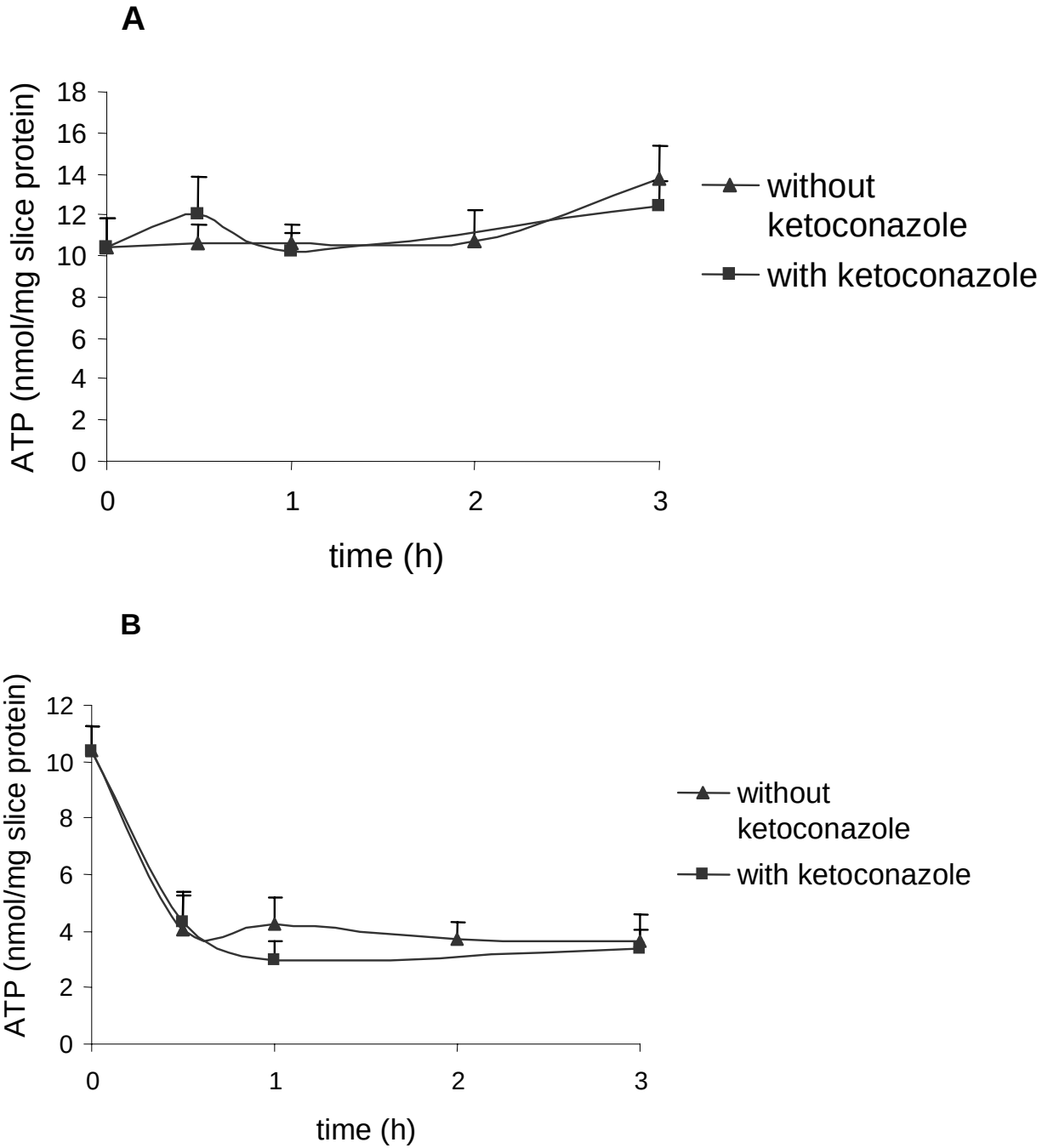

Figure 1

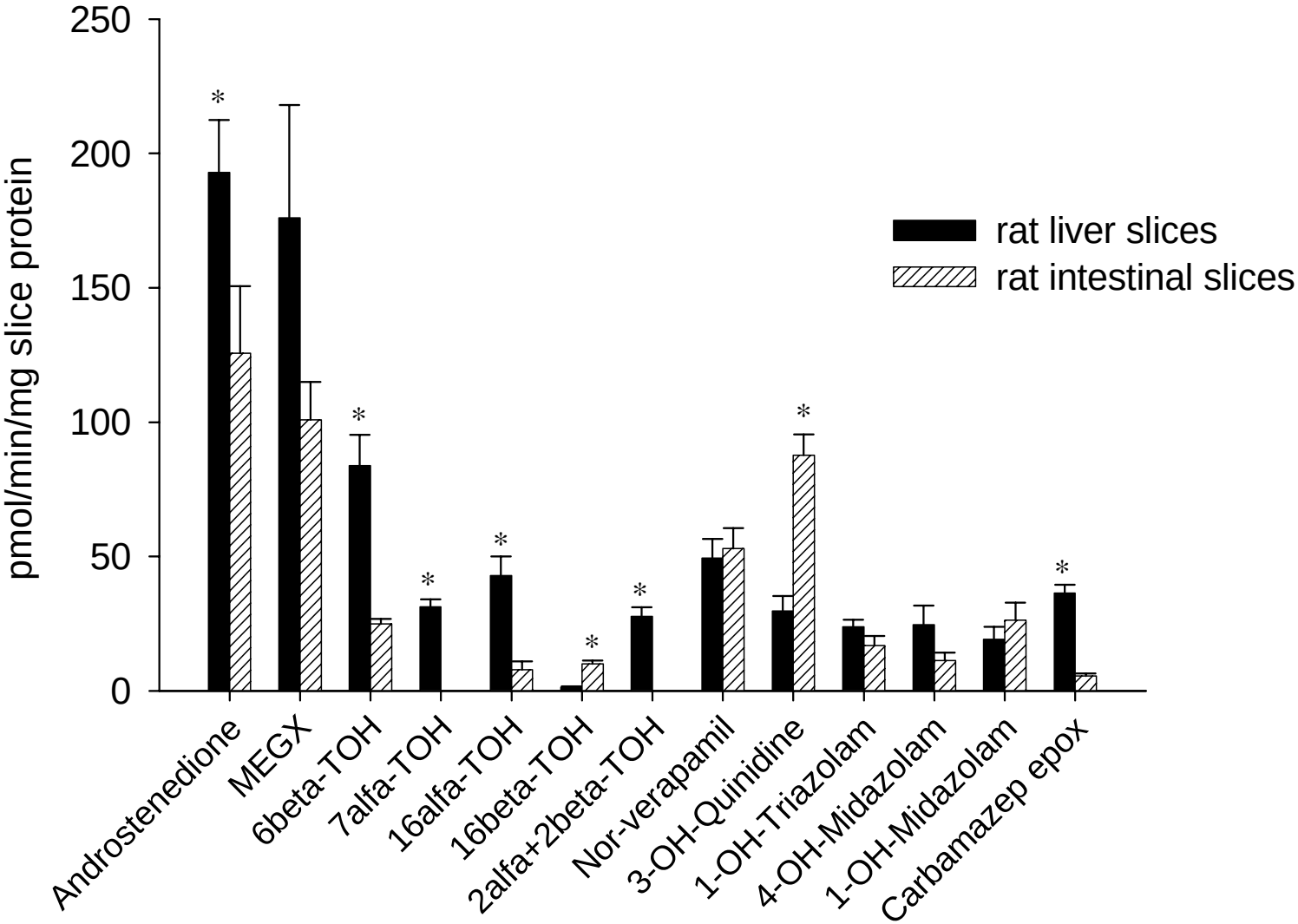

Figure 2A

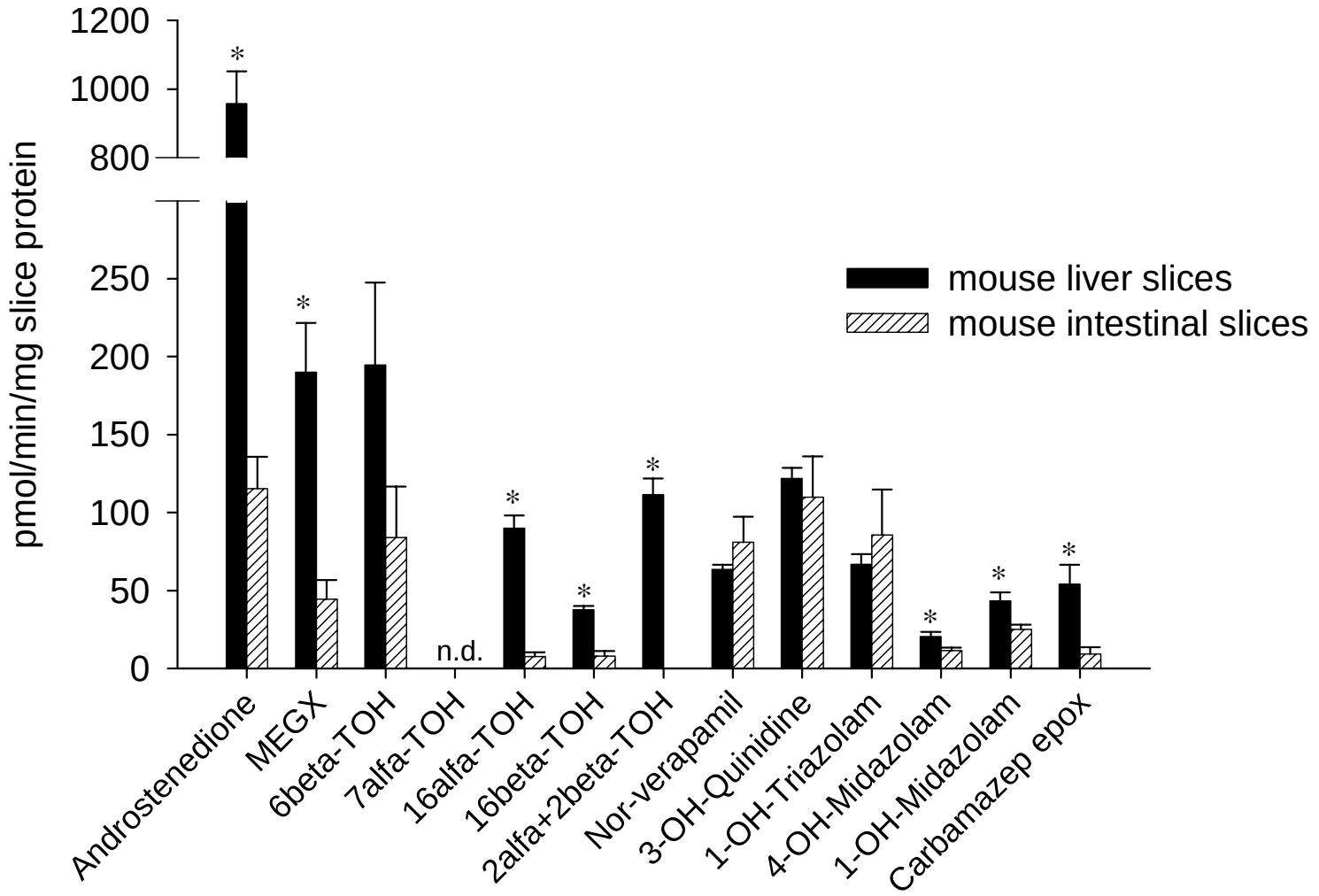

Figure 2B

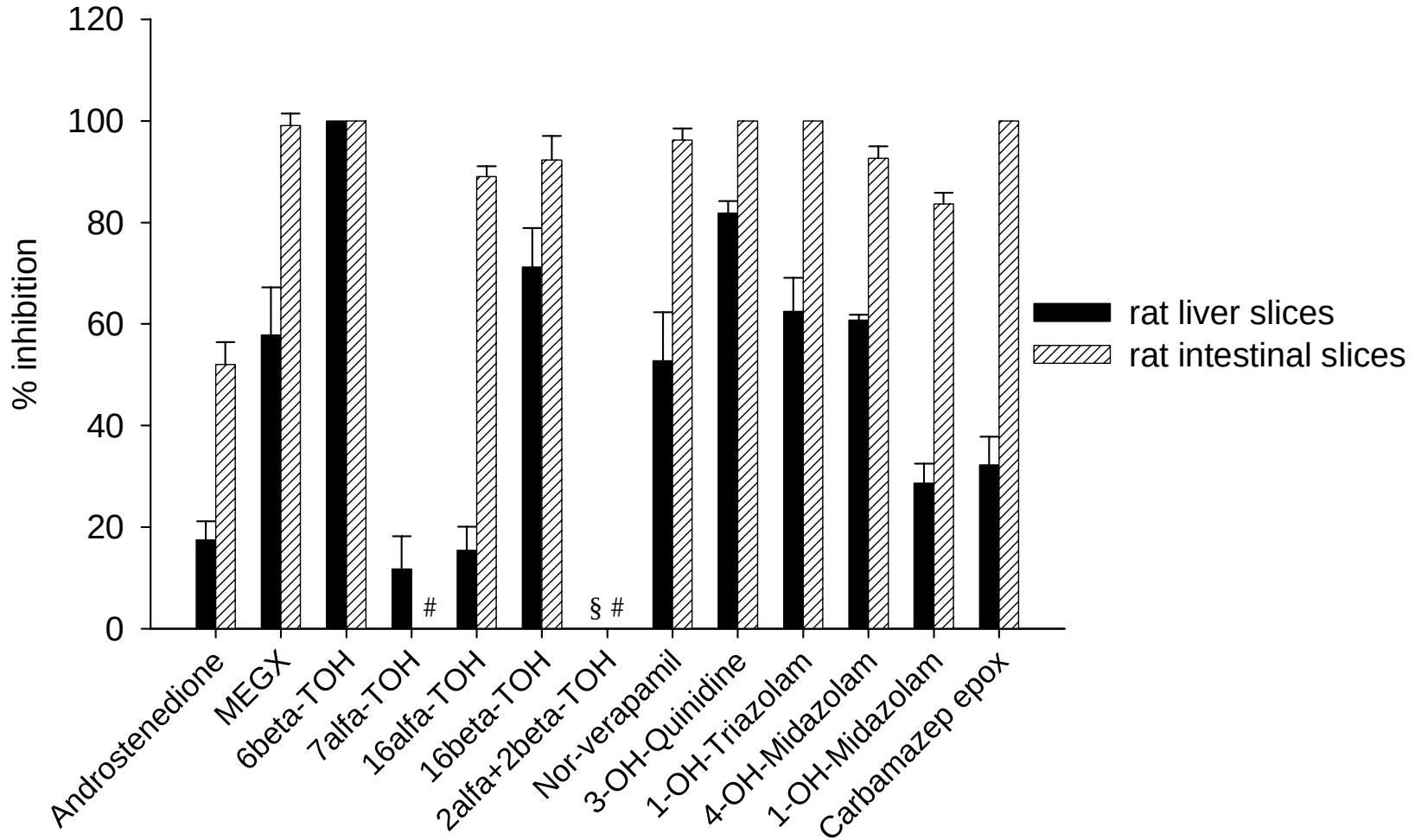

Figure 3A

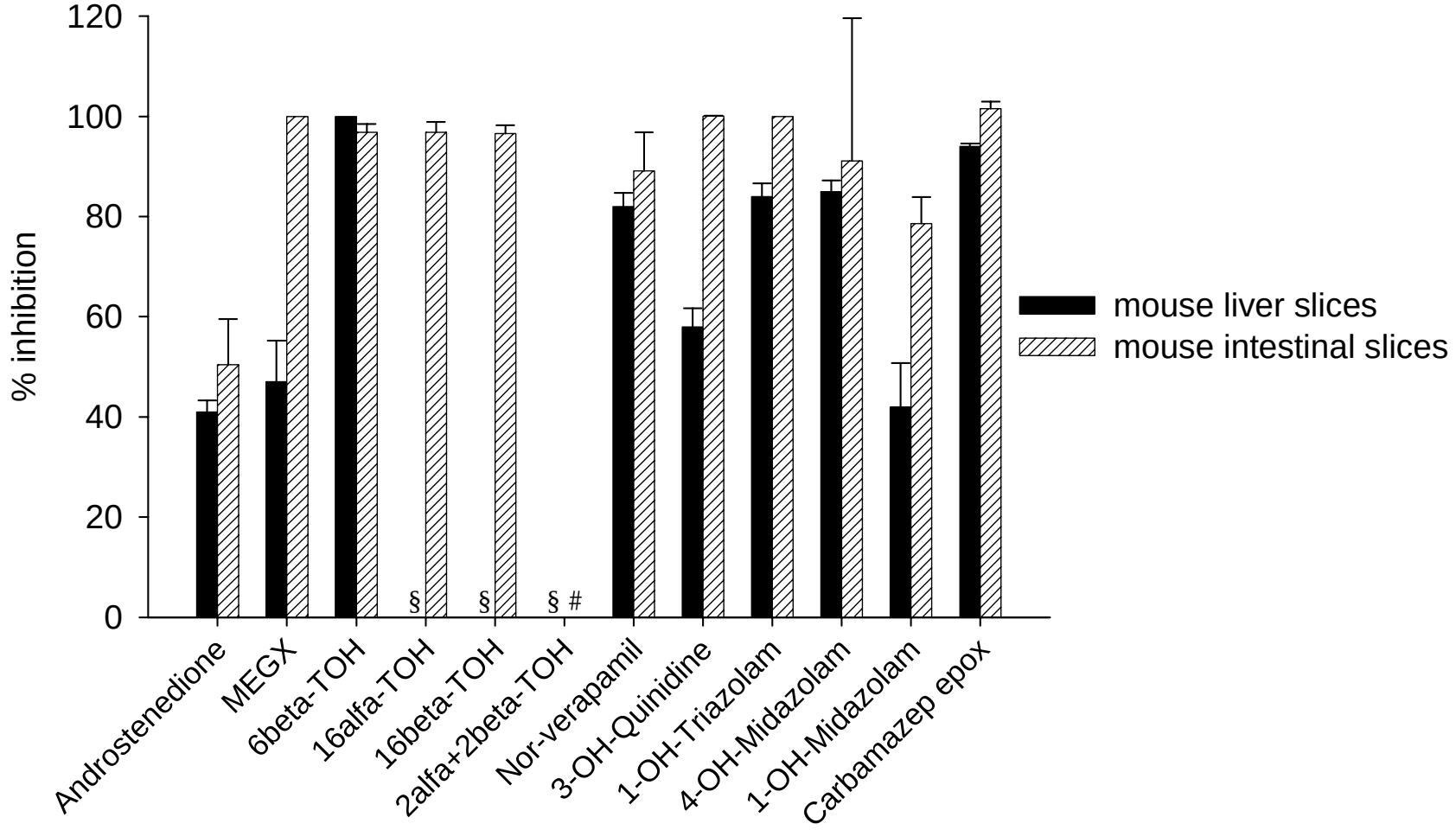

Figure 3B